Preparation and characterization of composite membranes composed of zirconium tricarboxybutylphosphonate and polybenzimidazole for intermediate temperature operation

Moon Yup Jang, Yohtaro Yamazaki*

Department of Innovative and Engineered Materials, Graduate School of Science and Engineering, Tokyo Institute of Technology, 4259 Nagatuta, Midori-ku, Yokohama, Kanagawa 226-8502, Japan

Abstract

Zirconium tricarboxybutylphosphonate, $Zr(O_3PC(CH_2)_3(COOH)_3)_2$, was synthesized by slowly decomposing zirconium fluoro-complexes in the presence of 2-phosphonobutane-1,2,4-tricarboxylic acid (PBTC) to prepare inorganic/organic composite membranes based on polybenzimidazole (PBI). Composite membranes composed of zirconium tricarboxybutylphosphonate (Zr(PBTC)) particles embedded in PBI were formed by evaporating the solvent from a suspension of Zr(PBTC) particles in a PBI solution. Composite membranes with 50 wt.% Zr(PBTC) exhibited uniform distribution of the particles throughout the thickness, as ascertained by scanning electron microscopy. The conductivities measured for compacted Zr(PBTC) powder and PBI-based membranes with 50 wt.% Zr(PBTC) were 6.74×10^{-2} and $3.82 \times 10^{-3}\,S\,cm^{-1}$, respectively, at 200 °C for $P_{H_2O}/P_s = 1$. Functionalization of the PBI with phosphoric acid groups obtained by treatment with phosphoric acid and with sulfonic acid groups obtained by post-sulfonation thermal treatment with sulfuric acid improved the proton conductivity of 50 wt.% Zr(PBTC) membranes to 5.24×10^{-3} and $8.14 \times 10^{-3}\,S\,cm^{-1}$ under the same measurement conditions. Zr(PBTC)/PBI membranes thus have great potential as proton exchange membrane fuel cells (PEMFCs).
© 2004 Published by Elsevier B.V.

Keywords: Zirconium tricarboxybutylphosphonate; Polybenzimidazole; Composite membrane; Intermediate temperature operation; SEM; PEMFCs

1. Introduction

Proton exchange membrane fuel cells (PEMFCs) that can operate at temperatures above 100 °C are receiving widespread attention [1–3] because operation at elevated temperatures reduces the adsorption of CO onto the platinum electrocatalyst and improves the electrode kinetics [4]. Also, they can reduce the polarization at the oxygen electrode, a major cause of the total voltage drop, and facilitate control of the water balance in the fuel cell system [5]. Thus, there have been various attempts to develop new electrolytic membranes that are stable at temperatures up to 150 °C and less expensive. They have taken two main approaches: functionalizing the thermostable polymers by introducing protogenic groups and fixing inorganic and inorganic–organic proton-conducting materials to be used as fillers in a binding polymer [6–8]. In the latter approach, the polymer is subsequently functionalized with acid groups to increase the conductivity of the final membrane.

A new class of organic derivatives of layered group IV phosphonates has recently been synthesized and structurally characterized. These compounds have the formula $M^{IV}(O_3PR)_2$, R being an organic group, and possess a structure similar to that of α-$Zr(HPO_4)_2\cdot H_2O$, with R groups replacing the OH ones and associate thermal and chemical stability of the inorganic matrix with the versatility of the organic part [9–11]. If R possesses an ionogenic group, such as $-SO_3H$, $-COOH$, or $-PO_3H$, the compound behaves as an inorganic–organic ion exchanger and exhibits ionic conductivity [12].

In our lab, zirconium tricarboxybutylphosphonate, $Zr(O_3PC(CH_2)_3(COOH)_3)_2$, was synthesized by decomposing zirconium fluoro-complexes in the presence of 2-phosphonobutane-1,2,4-tricarboxylic acid (PBTC). This

* Corresponding author. Tel.: +81 45 924 5411; Fax: +81 45 924 5433.
E-mail addresses: yamazaki@iem.titech.ac.jp (Y. Yamazaki).

compound behaves as an inorganic–organic ion exchanger with carboxylic groups attached to the insoluble crystalline inorganic matrix. The synthesized zirconium tricarboxy-butylphosphonate (hereafter Zr(PBTC)) was examined and found to be a good protonic conductor at 40–200 °C as a function of the relative humidity (RH). It was stable up to at least 200 °C, and its conductivity was of the order of $0.01\,S\,cm^{-1}$ at 100–200 °C at RH close to 100%. Due to the high conductivity of this compound, we decided to develop a composite membrane with a polymer binder—a mechanically resistant membrane with low gas permeability. The prepared Zr(PBTC) was in powdered form, so a binding polymer had to be introduced to form a membrane. Polybenzimidazole (PBI) was used as the binder agent due to its high thermal and thermo-oxidative stability, superior mechanical properties, and excellent chemical stability [13]. As it is an electrical insulator, when it is complexed with a strong inorganic acid such as sulfuric or phosphoric acid, it becomes proton conductive [14,15].

In this paper, we describe the preparation and characterization of a Zr(PBTC) compound and Zr(PBTC)/PBI membranes composed of Zr(PBTC) and PBI. We also report some important physico-chemical characteristics displayed by H_3PO_4-doped Zr(PBTC)/PBI membranes and by post-sulfonation thermal-treated Zr(PBTC)/PBI membranes. The membranes were doped with H_3PO_4 by immersing them into 11 mol/L H_3PO_4 solution. They were sulfonated using a method described in a US patent 4,634,530 for attaching a sulfonate group to the aromatic ring of PBI.

2. Experimental

2.1. Preparation of Zr(PBTC)compound

We prepared the Zr(PBTC) compound using a method similar to that of the corresponding zirconium compound described by Stein et al. [16]. We dissolved 6.45 g (0.02 mol) of $ZrOCl_2\cdot8H_2O$ in 30 ml of distilled deionized water and added 15 ml of 48% hydrofluoric acid to form a zirconium fluoro complex. We then added 0.04 mol of 2-phosphonobutane-1,2,4-tricarboxylic acid, $(OH)_2OPC(CH_2)_3(COOH)_3$, to the mixture at 80 °C. No precipitation occurred at this point because of the zirconium present as the fluoro complex. After heat treatment for 4 days, Zr(PBTC) powder precipitated. The precipitate was washed with distilled water until the pH of the filtrate exceeded 3.5. It was then dried in a desiccator for 4 days.

2.2. Preparation of membranes

We prepared the composite membranes using the previously prepared Zr(PBTC) compound as the inorganic proton conductor component. Using a procedure similar to that described by Staiti [17], we dispersed the proper amount of Zr(PBTC) powder in a small amount of water and then

added 1 N NaOH solution to neutralize the suspension. The suspension was evaporated, and the remaining powder was ground again. The neutralization of the suspension was necessary to prevent precipitation of the PBI when the inorganic compound was added to the polymer solution.

To obtain the solution needed to prepare the membranes, PBI in powder form (Aldrich Chemical Company, Inc.) was dissolved in *N,N*-dimethylacetamide (DMAc) at 150 °C for 15 h. The solution was subsequently filtered to eliminate any polymer particles from the suspension. The neutral Zr(PBTC) powder and PBI solution were mixed together with continuous stirring to form a homogeneous paste, which was then spread at a constant thickness on a smooth Petri dish and kept under solvent vapor at 60–70 °C for 24 h. The resulting membranes were separated from the bottom of the dish by adding water. They were then rinsed with distilled water and then treated with a 4 N HCl solution for 24 h to replace the sodium ions with protons. Finally, they were boiled for 1 h in distilled water.

Three types of membranes were prepared: 30, 50, and 70 wt.% Zr(PBTC) with the remainder PBI. The 50 wt.% type (hereafter Zr(PBTC)P50) had the highest proton conduction and mechanical stability. It was thus used as the target for preparing Zr(PBTC)/PBI membranes treated with phosphoric acid and sulfuric acid. We also prepared PBI membranes by dissolving PBI powder in DMAc, spreading the solution on a glass plate, and evaporating the solvent at 60–70 °C for 24 h.

2.3. Complexation of membranes

The Zr(PBTC)P50 membranes and of the PBI membranes were doped with H_3PO_4 by immersing them into 11 mol/L H_3PO_4 solution at room temperature for 24 h. They were then washed in boiling distilled water for 2 h and then dried at 50 °C for 24 h. The resulting membranes are referred to as Zr(PBTC)P50/H_3PO_4 and PBI/H_3PO_4 membranes. Both types were stored between filter paper in a hermetically sealed plastic bag at room temperature until they were used for characterization.

2.4. Sulfonation of membranes

The Zr(PBTC)P50 and PBI membranes were sulfonated using a method [18]. They were placed in a rectangular clamped metal frame for support and then immersed into 2.5 wt.% H_2SO_4 solution at 50 °C for 2 h. They were then rinsed in water and wiped to remove the water droplets. The membranes, still in the metal frame, were then placed in an oven at 480 °C for 60 s. The resulting membranes are referred to as Zr(PBTC)P50-S60 and sPBI membranes. About half of the Zr(PBTC)P50-S60 samples were washed in boiling water for 3 h and dried at 50 °C for 24 h; these membranes are referred to as Zr(PBTC)P50-S60w membranes.

2.5. Characterization of Zr(PBTC) compound and membranes

The X-ray diffraction (XRD) patterns of samples were collected using a Rigaku Rint 2000 diffractometer system and Cu Kα radiation. The Fourier transform infrared (FTIR) spectra of the samples were recorded between 2000 and 500 cm^{-1} using a Shimadzu FTIR-8700 spectrometer. Microanalyses of the C, H, Zr, and P were performed using a LECO CHNS–932 elemental analysis instrument and a Shimadzu ICPS 8100 sequential plasma spectrometer. Thermograms were recorded under a nitrogen atmosphere using a Rigaku Thermo Plus TG 8120 thermogravimetric-differential thermal analysis instrument at a heating rate of 10 °C min^{-1}. The morphologies of the Zr(PBTC) compound and the Zr(PBTC)P50 membranes were characterized using a JEOL 5600 scanning electron microscope (SEM).

2.6. Measurement of conductivity

The proton conductivity of samples of compacted Zr(PBTC) powder and membranes was measured using ac impedance spectroscopy at an oscillation amplitude of 100 mV in the frequency range 1.0–2.2 MHz. The compacted Zr(PBTC) powder, with a diameter of 12 mm and a thickness 1 mm, was prepared by hydrostatic pressing at 250 MPa. Platinum electrodes were deposited on both sides of the compacted Zr(PBTC) powder by RF sputtering. For measurements near room temperature, samples were placed in a thermostatic compartment to which a mixture of dry and water-saturated air at a specific ratio was introduced. The measurements were carried out at temperatures up to 200 °C in a specially designed stainless steel pressure vessel, in which the equilibrium pressure of water is 1.38 MPa. This experimental setup enabled the samples to equilibrate with saturated water vapor at the desired temperature. The resistance of the membranes was taken at the frequency that produced the minimum imaginary response [19].

3. Results and discussion

3.1. Characterization of Zr(PBTC) compound and membranes

Chemical analysis showed the Zr(PBTC) compound to be $Zr(O_3PC(CH_2)_3(COOH)_3)_2$. Experimental analysis showed the composition (%, w/w) to be 14.48% Zr, 9.86% P, 26.6% C, and 2.86% H. Calculation showed it to be 14.50% Zr, 9.88% P, 26.8% C, and 2.87% H.

The XRD patterns for the Zr(PBTC) compound and the PBI, Zr(PBTC)P50, Zr(PBTC)P50/H₃PO₄, and Zr(PBTC)P50-S60 membranes are shown in Fig. 1. That for the compound presented few broad peaks; the first reflection was generally (002), corresponding to an inter-
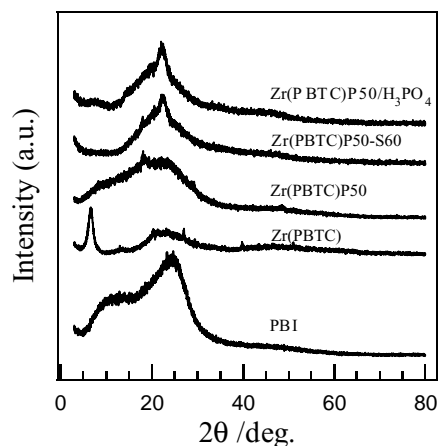

Fig. 1. X-ray diffraction patterns of Zr(PBTC) compound and PBI, Zr(PBTC)P50, Zr(PBTC)P50/H₃PO₄, and Zr(PBTC)P50-S60 membranes.

layer spacing of 13.1 Å. The interlayer spacing is difficult to determine accurately because Zr(PBTC) with terminal –COOH groups swells readily on exposure to air. The XRD pattern for a thoroughly dried Zr(PBTC) compound showed interlayer spacing reflection of 11.1 Å. The pattern for the PBI membrane showed a broad peak at $2\theta = 24°$, resulting from the convolution of amorphous and crystalline scattering. In the X-ray pattern of the Zr(PBTC)P50 membrane modified with Zr(PBTC), only a peak overlaid by the broad polymer reflection in the region of 2θ from 15 to 35 can be seen. The patterns of the H₃PO₄-doped membrane, Zr(PBTC)P50/H₃PO₄, and the post-sulfonation thermal-treated membrane, Zr(PBTC)P50-S60, showed an increase in the scattering intensity from the crystalline region with respect to the amorphous region. This indicates that as a consequence of the presence of hydrogen and $H_2PO_4^-/HSO_3^-$ groups along the polymeric chains of the PBI, inter-chain and intra-chain hydrogen bridge bondings formed that stimulated the formation of a more crystalline structure in the Zr(PBTC)P50 membrane. Bouchet and Siebert [20] demonstrated that the formation of hydrogen bridge bonds in a non-symmetric polymer increases the crystalline characteristics.

The infrared patterns of the Zr(PBTC) compound and of the PBI, Zr(PBTC)P50, Zr(PBTC)P50/H₃PO₄, Zr(PBTC)P50-S60, and Zr(PBTC)P50-S60w membranes are shown in Fig. 2 for 500–2000 cm^{-1}. The carboxylic acids of the compound were well assigned by the FTIR spectroscopy to regions near 1700, 1400, and 1250 cm^{-1} [21], so study of these regions reliably identifies these acids. The absorption near 1700 cm^{-1} is assigned to C=O stretching vibration. The two other absorptions, near 1400 cm^{-1} (1400–1395 cm^{-1}) and near 1250 cm^{-1} (1320–1210 cm^{-1}), have been associated by many researchers with single bond C–O stretching vibration [22]. The absorption spectrum of the Zr(PBTC)P50 membranes was almost the same as that of the PBI membranes for 500–2000 cm^{-1}, suggesting that the Zr(PBTC)P50 membranes were simply a mixture of
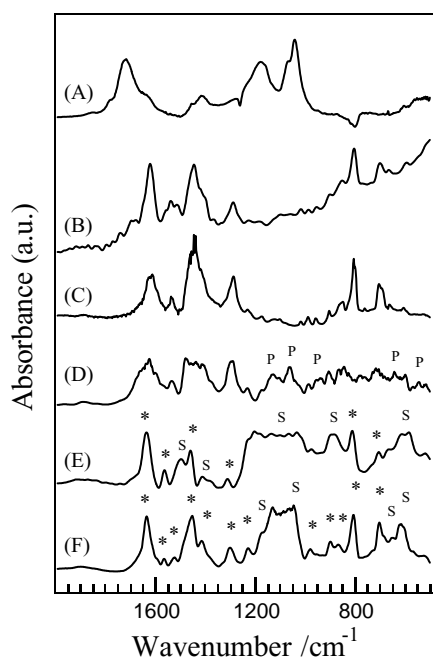
Fig. 2. FTIR spectra patterns of (A) Zr(PBTC) compound, (B) PBI, (C) Zr(PBTC)P50, (D) Zr(PBTC)P50/H_3PO_4, (E) Zr(PBTC)P50-S60, and (F) Zr(PBTC)P50-S60w membranes.

Fig. 3. Thermogravimetric weight loss curves of Zr(PBTC) compound and PBI, Zr(PBTC)P50, Zr(PBTC)P50/H_3PO_4, and Zr(PBTC)P50-S60 membranes.

Zr(PBTC) and PBI with no significant chemical interaction between them.

Investigation of Zr(PBTC)P50/H_3PO_4 revealed the characteristic absorption of H_3PO_4 molecules (labelled "P" in Fig. 2). Characteristic absorption of the HPO_4^{2-}, P–OH, and $H_2PO_4^-$ groups appears at 945, 1065, and 1135 cm^{-1}, respectively [23–26]. After post-sulfonation thermal treatment of the Zr(PBTC)P50 membranes, marked changes appeared in the spectra, although the main features of the PBI membranes (indicated by asterisks in Fig. 2) were still clearly observed in the spectrum of the Zr(PBTC)P50-S60 membrane. New bands (labelled "S" in Fig. 2) were observed in the 1000–1250 cm^{-1} region, indicating the presence of the grafted sulfonic acid group (HSO_3^-). The bands at 1042 and 1170–1228 cm^{-1} indicate symmetric and asymmetric vibrations of the sulfonate group, in agreement with Gieselman and Reynolds [27] who reported IR bands $\nu(SO_3)$ at 1040 and 1221 cm^{-1}. When the Zr(PBTC)P50-S60 membrane was boiled in water, the pattern characteristics of the Zr(PBTC)P50 membrane were not completely recovered in the spectrum of the Zr(PBTC)P50-S60w membrane. This could be due to the unbound sulfuric acid being absorbed by the membrane. The differences in the 600–700 cm^{-1} region could also be due to an increase in the number of C–S bonds in the thermally treated sample [28].

Thermogravimetric analysis was carried out between 25 and 800 °C. As shown in Fig. 3, for the Zr(PBTC) compound, there were three distinct regions of weight loss with the increase in temperature. Using quantity calculation of the weight loss in each region, we identified the
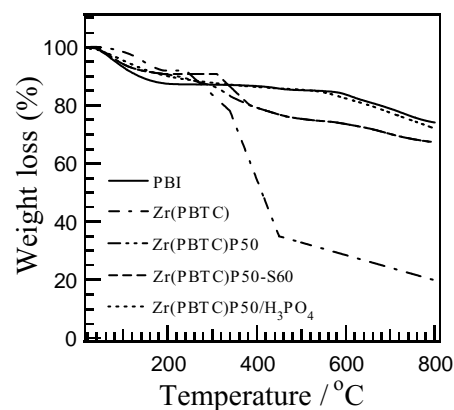
corresponding thermal decomposition processes. The first weight loss, up to 190 °C, is associated with interlayer water loss. The second one, from 250 to 340 °C, represents the decomposition of CH_2 organic components. The strong weight loss region from 340 to 450 °C is related to the complete decomposition of the carboxyl groups. As shown in Fig. 3, the Zr(PBTC)P50 membrane was more stable than the Zr(PBTC) compound—there was a weight loss region starting at about 320 °C. It is thus likely that an increase in thermal stability arises from good interfacial contacts between the polymer and the filler particles. The Zr(PBTC)P50/H_3PO_4 and Zr(PBTC)P50-S60 membranes were more thermally stable than the Zr(PBTC)P50 membrane. These results suggest that modifying the Zr(PBTC)P50 membrane with H_3PO_4 and H_2SO_4 leads to the formation of rather strong hydrogen bonding. Moreover, the H_3PO_4 makes Zr(PBTC)/PBI membranes more thermally stable than Zr(PBTC)/PBI membranes sulfonated by H_2SO_4.

3.2. Evaluation of conductivity

The proton conductivity versus temperature results for the Zr(PBTC) compound and the Zr(PBTC)P50, PBI/H_3PO_4, and Zr(PBTC)P50/H_3PO_4 membranes at 40–200 °C at 100% RH are shown in Fig. 4. The conductivity for the compound extended over the range 10^{-3} to 10^{-2} S cm^{-1} with increasing temperature. The maximum conductivity was 6.74 × 10^{-2} S cm^{-1} at 200 °C. The conductivity for the PBI/H_3PO_4 membrane extended over the range 10^{-5} to 10^{-4} S cm^{-1} with increasing temperature. The maximum conductivity was 3.84 × 10^{-4} S cm^{-1} at 200 °C. The Zr(PBTC)P50 membrane had a conductivity of 3.82 × 10^{-3} S cm^{-1} at 200 °C. The functionalized Zr(PBTC)P50/H_3PO_4 membrane had higher conductivity than the non-treated one. The Zr(PBTC)P50/H_3PO_4 membrane had a maximum conductivity of 5.24 × 10^{-3} S cm^{-1} at 200 °C. Based on the IR results reported by Bouchet and Siebert [20] on the
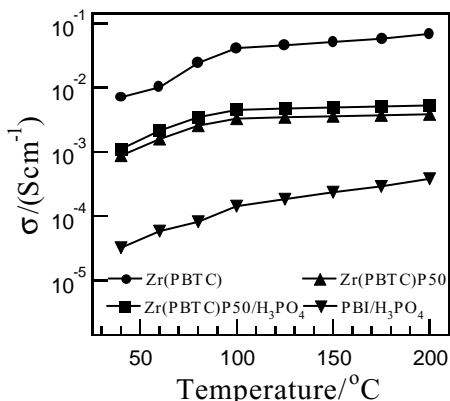
Fig. 4. Plots of conductivity (σ) vs. temperature for compacted Zr(PBTC) powder and Zr(PBTC)P50, PBI/H$_3$PO$_4$, and Zr(PBTC)P50/H$_3$PO$_4$ membranes at 100% RH.
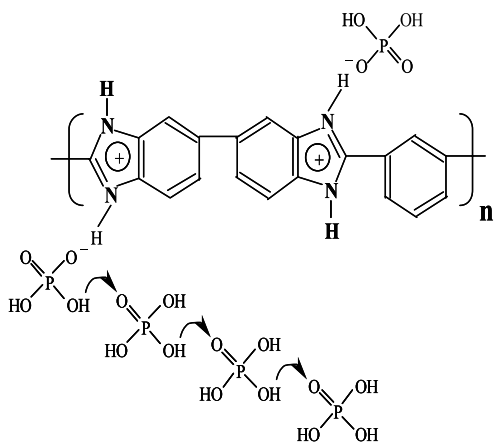

Fig. 5. Schematic representation of proton conduction paths between PBI and H$_3$PO$_4$.

protonation of the nitrogen of imidazole by H$_3$PO$_4$ in the 2500–3000 cm^{-1} region, this increasing conductivity phenomenon suggests that the mixing of the Zr(PBTC)P50 membrane with H$_3$PO$_4$ leads to the protonation of two imidazole groups of a PBI unit with the presence of H$_2$PO$_4^-$.
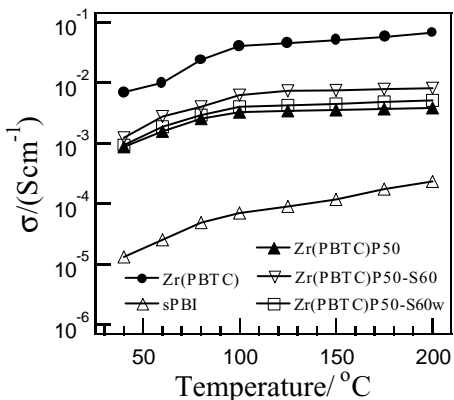

Fig. 6. Plots of conductivity (σ) vs. temperature for compacted Zr(PBTC) powder and Zr(PBTC)P50, sPBI, Zr(PBTC)P50-S60, and Zr(PBTC)P50-S60w membranes at 100% RH.

It also suggests that the exchange of protons among excess H$_3$PO$_4$ molecules linked to the H$_2$PO$_4^-$ rather by strong hydrogen bonding improves proton conductivity of Zr(PBTC)P50 membrane (see Fig. 5).

The proton conductivity versus temperature results for the Zr(PBTC) compound and the Zr(PBTC)P50, sPBI, Zr(PBTC)P50-S60, and Zr(PBTC)P50-S60w membranes at 40 to 200 °C at 100% RH are shown in Fig. 6. As mentioned above, the highest conductivities for the compound and the Zr(PBTC)P50 membrane were 6.74×10^{-2} and 3.82×10^{-3} S cm^{-1}, respectively. The low conductivity of the sPBI membrane may have been due to the low de-
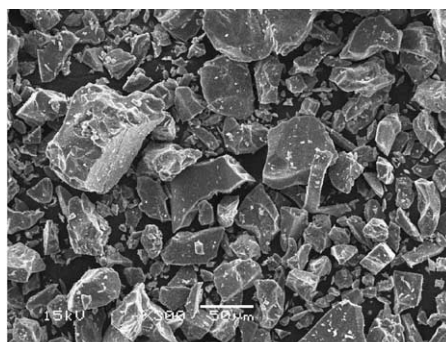
(a) Magnification: × 300
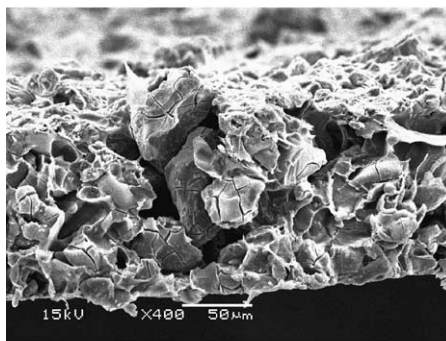
(b) Magnification: × 400
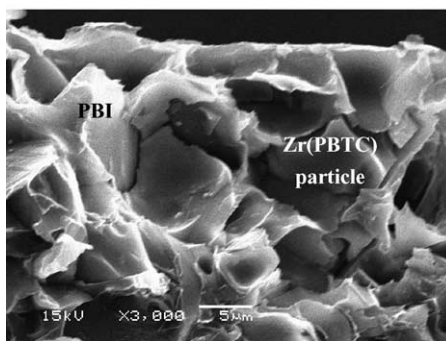
(c) Magnification: × 3000

Fig. 7. SEM photographs of (a) Zr(PBTC) particles and (b, c) a cross-section of Zr(PBTC)P50 membrane. Magnification: (a) 300×; (b) 400×; (c) 3000×.

gree of sulfonation and to the small number of protons available for transport because only the acid protons are strongly bonded to the imide ring; the highest conductivity was $2.34 \times 10^{-4}\,\mathrm{S\,cm^{-1}}$ at $200\,^{\circ}\mathrm{C}$. The conductivity of the sPBI membranes was similar to that reported by Staiti et al. [29] and much lower than those obtained by Glipa et al. [30] on grafted methyl benzenesulfonate membranes ($1 \times 10^{-2}\,\mathrm{S\,cm^{-1}}$ at $40\,^{\circ}\mathrm{C}$ and 100% RH). This could be due to the different characteristics of the functional groups (sulfonate and methyl benzenesulfonate) and to the methods of performing the conductivity measurements. For the Zr(PBTC)P50-S60 membrane, the maximum conductivity was $8.14 \times 10^{-3}\,\mathrm{S\,cm^{-1}}$ at $200\,^{\circ}\mathrm{C}$. After being washed, the conductivity of the Zr(PBTC)P50-S60 membrane decreased due to the removal of the ionically bonded acid. The highest conductivity of the Zr(PBTC)P50-S60w membrane was $5.10 \times 10^{-3}\,\mathrm{S\,cm^{-1}}$ at $200\,^{\circ}\mathrm{C}$.

3.3. Structure of Zr(PBTC) compound and Zr(PBTC)P50 membrane

SEM was used to characterize the structural morphologies of the Zr(PBTC) compound and the Zr(PBTC)P50 membrane. As shown by the SEM photomicrograph in Fig. 7(a), the structural framework of the compound was highly crystalline with a heteromorphous geometry. As shown by the one in Fig. 7(b), the membrane with 50 wt.% Zr(PBTC) had a uniform distribution of the Zr(PBTC) particles throughout its thickness. They were covered with a layer of PBI, and some had surface cracks. Since the sputtering and SEM inspection were carried out under high vacuum conditions, the PBI might have become completely dry, causing the particles to shrink and crack. The higher magnification image of the same sample in Fig. 7(c) shows that the PBI was concentrated in the inter-granular regions between the particles. Based on these results, the protons must have diffused to the surface of the particles by a grain boundary mechanism and the treatments to make PBI with proton conductivity characteristics must have influenced positively the proton conductivity of Zr(PBTC)P50 membranes.

4. Conclusion

The introduction of well-dispersed hydrophilic nanoparticles into polymers, replacing the expensive Nafion membrane, might improve the mechanical characteristics of the membranes and reduce the reactant crossover from the anodic to the cathodic region by influencing their hydrophilic interconnections [31]. A promising inorganic material for composite membranes is Zr(PBTC). Our experiments showed that the highest conductivity using compacted Zr(PBTC) powder is $0.0674\,\mathrm{S\,cm^{-1}}$ at $200\,^{\circ}\mathrm{C}$ for $P_{\mathrm{H_2O}}/P_s = 1$. Pure PBI is an insulator with an intrinsic conductivity of about $10^{-12}\,\mathrm{S\,cm^{-1}}$ at $25\,^{\circ}\mathrm{C}$. When Zr(PBTC) particles were mixed with PBI, they acted as proton carriers

and increased proton conductivity in the membrane. There are a number of hydrogen bonds among the COOH, PBI, and water molecules in Zr(PBTC)/PBI membranes. The addition of Zr(PBTC) not only provides more protons but also facilitates their transport. The Zr(PBTC)P50 membranes were mechanically stable and had a proton conductivity of $3.82 \times 10^{-3}\,\mathrm{S\,cm^{-1}}$ at $200\,^{\circ}\mathrm{C}$ for $P_{\mathrm{H_2O}}/P_s = 1$. Proton conduction in the Zr(PBTC)P50 membrane was further improved by functionalizing the PBI with phosphonic acid groups obtained by treatment with phosphoric acid and with sulfonic acid groups obtained by post-sulfonation thermal treatment. The Zr(PBTC)P50/H_3PO_4 and Zr(PBTC)P50-S60 membranes had proton conductivities of 5.24×10^{-3} and $8.14 \times 10^{-3}\,\mathrm{S\,cm^{-1}}$ under the same measurement conditions. Although the Zr(PBTC)P50-S60 membrane retained acid molecules after washing, its proton conductivity was lower due to the removal of the ionically bonded acids. The proton conductivity might be further improved by repeating the post-sulfonation thermal treatment more than once, as described by Kuder and Chen [18]. From our results, we conclude that Zr(PBTC)/PBI membranes modified with H_3PO_4 and H_2SO_4 have great potential as electrolytic membranes. We are now investigating methods for preparing membrane/electrode assemblies to assess the viability of these membranes as proton exchange membrane fuel cells.

References

[1] J. Kerres, A. Ullrich, Th. Harring, M. Baldauf, U. Gebhardt, W. Preidel, J. New Mater. Electrochem. Syst. 3 (2000) 129.

[2] J.T. Wang, R.F. Savinell, J.S. Wainright, M. Litt, H. Yu, Electrochim. Acta 41 (1996) 193.

[3] M. Kawahara, J. Morita, M. Rikukawa, K. Sanui, N. Ogata, Electrochim. Acta 45 (2000) 1395.

[4] H.F. Oetjen, V.M. Schmidt, U. Stimming, F. Trila, J. Electrochem. Soc. 143 (1996) 3838.

[5] Y.M. Li, M. Hibino, M. Miyayania, T. Kudo, Solid State Ionics 134 (2000) 271.

[6] P. Staiti, S. Freni, S. Hocevar, J. Power Sources 79–2 (1999) 250.

[7] G. Alberti, M. Casciola, Solid State Ionics 97 (1997) 177.

[8] B. Bonnet, J. Jones, J. Roziere, L. Tchicaya, G. Alberti, M. Casciola, L. Massinelli, B. Bauer, A. Peraio, E. Ramunni, J. New Mater. Electrochem. Syst. 3 (2000) 87.

[9] G. Alberti, U. Costantino, S. Allulli, N. Tomassini, J. Inorg. Nucl. Chem. 40 (1978) 1113.

[10] G. Alberti, U. Costantino, M.L. Luciani, J. Chromatogr. 180 (1979) 45.

[11] M.B. Dines, P.M. Di Giacomo, Inorg. Chem. 20 (1981) 92.

[12] G. Alberti, in: P.A. Williams, M.J. Hudson (Eds.), Recent Developments on Ion Exchange, Elsevier, Amsterdam, 1987.

[13] S.R. Samms, S. Wasmus, R.F. Savinell, J. Electrochem. Soc. 143 (4) (1996) 1225.

[14] J.S. Wainright, J.T. Wang, D. Weng, R.F. Savinell, M. Litt, J. Electrochem. Soc. 143 (7) (1996) L121.

[15] X. Glipa, M. El Addad, D. Jones, J. Roziere, Solid State Ionics 98 (1997) 323.

[16] E.W. Stein, A. Clearfield, M.A. Subramanian, Solid State Ionics 83 (1996) 113.

[17] P. Staiti, J. New Mater. Electrochem. Systems 4 (2001) 181.

[18] J.E. Kuder, J.C. Chen, US patent 4,634,530, 1987.

[19] T.E. Springer, T.A. Zawodzinski, M.S. Wilson, S. Gottesfeld, J. Electrochem. Soc. 143 (1996) 587.

[20] R. Bouchet, E. Siebert, Solid State Ionics 118 (1999) 287.

[21] R.M. Silverstain, G.C. Bassier, T.C. Morril, Spectrometric Identification of Organic Compounds, John Wiley and Sons, Inc., 3rd ed., 1974.

[22] L.J. Bellamy, The Infrared Spectra of Complex Molecules, John Willey and Sons, New York, 1954.

[23] M.F. Daniel, B. Desbat, F. Cruege, O. Trinuet, J.C. Lassegues, Solid State Ionics 28–30 (1998) 637.

[24] R. Tanaka, H. Yamamoto, S. Kawamura, T. Iwase, Electrochim. Acta 40 (1995) 2421.

[25] W. Wieczorek, J.R. Stevens, Polymer 38 (1996) 2057.

[26] J.R. Steven, W. Wieczork, D. Randucha, K.R. Jeffrey, Solid State Ionics 97 (1997) 347.

[27] M.B. Gieselman, J.R. Reynolds, Macromolecules 25 (1992) 4832.

[28] B.C. Johnson, I. Yilgor, C. Tran, M. Iqbal, J.P. Wightman, D.R. Lloyd, J.E. McGrath, J. Polymer Sci. Polymer Chem. 22 (1984) 721.

[29] P. Staiti, F. Lufrano, A.S. Arico, E. Passalacqua, V. Antonuccci, J. Membr. Sci. 188 (2001) 71.

[30] X. Glipa, M. El Haddad, D.J. Jones, J. Roziere, Solid State Ionics 97 (1997) 323.

[31] J. Kj´ær, S. Yde-Andersen, N.A. Knudsen, E. Skou, Solid State Ionics 46 (1991) 169.